AD-A191 604 PHOTOIONIZATION DYNAMICS AND ABUNDANCE PATTERNS IN LASER VAPORIZED TIN AN..(U) GEORGIA UNIV ATHENS DEPT OF CHEMISTRY K LAIHING ET AL. 15 SEP 87 ARO-21703.8-CH 1/1

UNCLASSIFIED DAAG29-85-K-0040 F/G 7/2 NL

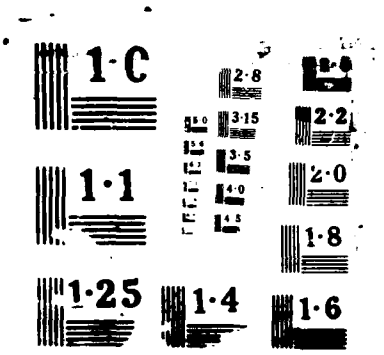
1·C
1·1
1·25
2·8
3·15
3·5
4·0
4·5
2·2
2·0
1·8
1·4
1·6

UNCLASSIFIED — FOR REPRODUCTION PURPOSES

SECURITY CLASSIFICATION

AD-A191 604

DTIC FILE COPY

UMENTATION PAGE

1a. REPORT SECUR: Uncla;	1b. RESTRICTIVE MARKINGS
2a. SECURITY CLAS: ...THORITY	3. DISTRIBUTION/AVAILABILITY OF REPORT: Approved for public release; distribution unlimited.
2b. DECLASSIFICATION/DOWNGRADING SCHEDULE	
4. PERFORMING ORGANIZATION REPORT NUMBER(S)	5. MONITORING ORGANIZATION REPORT NUMBER(S): ARO 21783.8-CH
6a. NAME OF PERFORMING ORGANIZATION: University of Georgia; 6b. OFFICE SYMBOL (If applicable)	7a. NAME OF MONITORING ORGANIZATION: U. S. Army Research Office
6c. ADDRESS (City, State, and ZIP Code): University of Georgia, Athens, GA 30602	7b. ADDRESS (City, State, and ZIP Code): P. O. Box 12211, Research Triangle Park, NC 27709-2211
8a. NAME OF FUNDING/SPONSORING ORGANIZATION: U. S. Army Research Office; 8b. OFFICE SYMBOL (If applicable)	9. PROCUREMENT INSTRUMENT IDENTIFICATION NUMBER: DAAG29-85-K-0040
8c. ADDRESS (City, State, and ZIP Code): P. O. Box 12211, Research Triangle Park, NC 27709-2211	10. SOURCE OF FUNDING NUMBERS: PROGRAM ELEMENT NO. / PROJECT NO. / TASK NO. / WORK UNIT ACCESSION NO.

11. TITLE (Include Security Classification)

Photoionization Dynamics and Abundance Patterns in Laser Vaporized Tin and Lead Clusters

12. PERSONAL AUTHOR(S)

K. Laihing, R. G. Wheeler, W. L. Wison and M.A. Duncan

13a. TYPE OF REPORT	13b. TIME COVERED	14. DATE OF REPORT (Year, Month, Day)	15. PAGE COUNT
Reprint	FROM _____ TO _____		

16. SUPPLEMENTARY NOTATION

The view, opinions and/or findings contained in this report are those of the author(s) and should not be construed as an official Department of the Army position, policy, or decision, unless so designated by other documentation.

17. COSATI CODES		
FIELD	GROUP	SUB-GROUP

18. SUBJECT TERMS (Continue on reverse if necessary and identify by block number)

19. ABSTRACT (Continue on reverse if necessary and identify by block number)

Abstract on reprint

DTIC ELECTE FEB 02 1988 S E

Accession For
NTIS GRA&I [X]
DTIC TAB [ ]
Unannounced [ ]
Justification
By
Distribution/
Availability Codes
Dist | Avail and/or Special
A-1 | 20

20. DISTRIBUTION/AVAILABILITY OF ABSTRACT	21. ABSTRACT SECURITY CLASSIFICATION	
☐ UNCLASSIFIED/UNLIMITED ☐ SAME AS RPT. ☐ DTIC USERS	Unclassified	
22a. NAME OF RESPONSIBLE INDIVIDUAL	22b. TELEPHONE (Include Area Code)	22c. OFFICE SYMBOL

DD FORM 1473, 84 MAR — 83 APR edition may be used until exhausted. All other editions are obsolete.

SECURITY CLASSIFICATION OF THIS PAGE

UNCLASSIFIED

Photoionization dynamics and abundance patterns in laser vaporized tin and lead clusters

K. LaiHing, R. G. Wheeler, W. L. Wilson, and M. A. Duncan
Department of Chemistry, School of Chemical Sciences, University of Georgia, Athens, Georgia 30602

(Received 24 April 1987; accepted 2 June 1987)

Tin and lead clusters are produced by laser vaporization in a pulsed nozzle source and studied with laser photoionization mass spectroscopy. "Magic numbers" are observed in both cluster size distributions under a variety of laser wavelength and power conditions which can be understood in terms of ionization thresholds, relative ionization cross sections, and multiphoton-induced fragmentation. After investigation of the photoionization dynamics, relative abundances of different sized clusters are estimated. Abundance patterns of tin and lead clusters are compared to those reported previously for other group IV elements (C, Si, Ge) to investigate the role of periodicity in cluster growth and bonding properties. Especially abundant 10-atom cluster species are observed for both tin and lead, as has been observed previously for both silicon and germanium. Other features not observed for silicon and germanium, such as abundance patterns characteristic of atom closepacking geometries, are observed to a limited degree for tin clusters and are more prominent in lead clusters.

INTRODUCTION

Since the development of new techniques producing gas phase metal clusters,[1,2] mass spectroscopy has been one of the primary tools used to probe size dependent cluster properties. Examples of mass spectroscopy cluster experiments include measurements of size distributions,[1-6] size dependent chemical reactivity,[7-9] and physical properties such as ionization potentials[10] and electron affinities.[11] In measurements of cluster abundances, local maxima or minima in cluster sizes are frequently encountered and have been referred to as "magic numbers."[12] However, the origin of these patterns is not well understood and has been the subject of some controversy.[12,13] Abundances may be influenced by a variety of factors, such as the mechanism of metal vaporization, the kinetics of cluster nucleation and growth,[14] the thermodynamic stability of the clusters formed, or fragmentation patterns in electron impact or photoionization detection. Any conclusions drawn from mass spectral data, therefore, must include a consideration of all these factors.

In this report we describe laser photoionization mass spectra of tin and lead clusters produced by laser vaporization in a pulsed nozzle source. These same cluster systems have been studied previously, formed by inert gas condensation in oven/beam sources and detected with electron impact ionization.[2,4,5] By comparison to these earlier experiments, this study examines magic number patterns in clusters of the same elements produced and detected under different conditions. As another motivation, recent photoionization studies have shown strong similarities between main group cluster elements having the same valence electron shell structure.[6,15] In particular, this has been observed for antimony and bismuth[15] as well as for silicon and germanium.[6] This study of tin and lead completes the series of photoionization studies for the group IVA elements and provides one of the first views of periodic cluster properties.

Surprisingly, these experiments using laser vaporization and UV laser photoionization techniques reproduce the tin and lead abundance patterns observed previously using oven/beam technology and electron impact ionization.[2,4,5] However, not all the features observed in the electron impact experiments are produced under the same set of laser photoionization conditions. The dependence of photoionization spectra on laser power and wavelength and the comparison to electron impact spectra suggest that both laser vaporization and oven/beam sources produce essentially the same size distribution of neutral clusters. Moreover, the distributions produced for lead and tin clusters are very similar. However, our results suggest that both electron impact and laser photoionization may distort the distribution observed mass spectrometrically depending on the specific conditions chosen, with contributions arising from either abundant neutral clusters or cation fragments. When studied under the same photoionization conditions, lead and tin exhibit significant similarities to silicon and germanium clusters.[6] The similarities in isoelectronic clusters and the fact that these patterns arise when clusters are produced by different techniques suggests that thermodynamic stability may play an important role in cluster growth for these elements. The abundance patterns observed can be rationalized in terms of covalent-like bonding arrangements as well as atomic close-packing structures. The importance of close-packing relative to bonding patterns progresses toward and is most pronounced for lead clusters, following a trend similar to that in the solid state structures of these same elements.

EXPERIMENTAL

The laser vaporization cluster source used in these experiments is similar to that reported in previous studies of metal clusters.[1,15] Our version of this source is shown in Fig. 1. It consists of a double solenoid pulsed nozzle (Newport Corporation BV-100) operating with 6 atm backing pres-

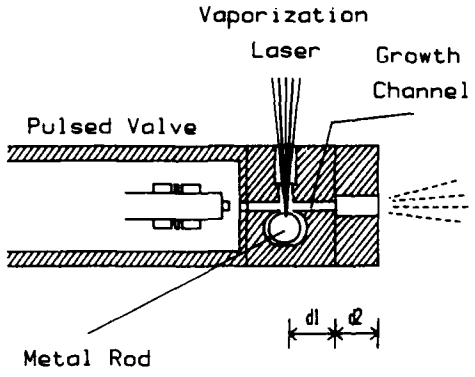

FIG. 1. Pulsed nozzle laser vaporization cluster source used for these experiments.

sure of helium, a 1 mm orifice diameter, and a 200 μs pulse duration at a 10–20 Hz repetition rate. Vaporization is accomplished by a focused ($\sim$1 mm spot) excimer laser (Lumonics 860) operating at either 193, 248, or 308 nm. Samples are prepared by melting pellets of the pure metals into a test-tube mold to produce a 0.5 in. diam rod. Vaporization occurs within a housing attached to the nozzle faceplate where the pulsed helium flow is confined to a 2 mm diam channel over the sample rod surface. After the vaporization laser pulse, which produces a hot metal-containing plasma, collisional energy transfer with excess helium cools the metal vapor to near room temperature and clusters grow in the channel (also 2 mm diam) extending beyond the vaporization point (section d1 in Fig. 1). The length of the growth region can be varied from 5 to 50 mm by addition of modular channel segments. An additional section of channel (4 mm diam $\times$ 10 mm long) is also added at the end of the growth region (section d2 in Fig. 1). While some additional cluster growth may occur here, the primary purpose of this section is to spread the cluster packet (via turbulent flow) to lessen the timing constraints on downstream detection.

The metal cluster/helium mixture expands freely out of the pulsed source into a vacuum system described previously[18] where it is collimated into a beam by a skimmer before entering the differentially pumped detection chamber. Photoionization is accomplished by a second excimer laser crossing the molecular beam in the source region of a homemade time-of-flight mass spectrometer. Positive ion mass spectra are processed with a Camac-based 100 MHz transient digitizer connected to an averaging memory module (Transiac 2101 system). The digitizer system is computer controlled (DEC PRO-350 computer) via an IEEE-488 bus and LeCroy 8901A Camac crate controller. Typical mass spectra reported are accumulated for 500 laser shots to average out pulse-to-pulse fluctuations in laser power or nozzle output.

Photoionization conditions

Ideally, mass spectral abundances should measure neutral cluster concentration as a function of size without the influences of varying ionization efficiency or fragmentation. However, these conditions are rarely realized because of size dependent ionization potentials, wavelength dependent cross sections, and multiphoton-induced fragmentation. In the case of tin and lead clusters, only limited information is available on size dependent ionization potentials.[19] And, by comparison to other cluster systems, multiphoton absorption and fragmentation are expected to be efficient,[20,21] making spectral intensities extremely sensitive to ionization laser conditions. Therefore, extensive power dependence studies at a variety of wavelengths are necessary to understand abundance patterns in these systems.

In the limit of low laser power it should be possible to eliminate, or at least limit, multiphoton absorption processes. Under the resulting single photon absorption conditions, ion signal intensities should vary linearly with the laser power. However, a linear power dependence does not necessarily indicate a single photon process. Linear power dependences may also result from multiphoton processes when some transitions are saturated. In laser photoionization mass spectroscopy, a more valid criterion for single photon absorption is that relative peak intensities do not change with further reduction in laser power. If these limiting low power conditions can be established, wavelength dependent studies can be used to probe cluster ionization potentials. Once thresholds are established, single photon absorption just above threshold will limit fragmentation (parent ion production is dominant). However, ionization cross sections may vary significantly near threshold, providing another unwanted influence on peak intensities. This effect can only be accounted for with wavelength dependent studies. If threshold cross section effects and fragmentation can be avoided, low power photoionization should provide a reasonably accurate measure of size dependent neutral cluster concentrations. We define these conditions as "neutral sensitive" photoionization conditions, which may or may not be realized in any particular experiment.

In the other extreme, moderate to high laser powers, especially at longer wavelengths, may cause extensive multiphoton absorption and fragmentation. Under these conditions only stable fragment ions survive further fragmentation and mass spectral abundances should favor stable cluster cations. However, depending on the dissociation mechanism, cluster cation stability toward fragmentation at a particular wavelength may not be the same as global thermodynamic stability. Therefore, highly fragmented cluster distributions should be interpreted with some caution.

In experiments described here, photoionization laser powers are varied over 2–3 orders of magnitude for the excimer laser wavelengths 248 (KrF), 193 (ArF), and 157 nm (F_2). High power conditions are typically 10 mJ/cm^2 for KrF or ArF lasers and 1 mJ/cm^2 for the F_2 laser. Low power limits for lead and tin clusters, below which relative intensities do not change, were observed between 0.1 and 0.02 mJ/cm^2.

RESULTS AND DISCUSSION

Cluster production

Mass spectra of tin and lead clusters under various conditions are shown in Figs. 2–7 and 9–10. We have produced

tin clusters up to 30–35 atoms and lead clusters up to 50–55 atoms. As might be expected, vaporization of these metals is relatively easy at all vaporization wavelengths used (193, 248, and 308 nm). In fact, these metals form clusters under milder laser and nozzle conditions than any of a variety of transition metals studied previously in our laboratory. Cluster size distributions depend on source parameters in much the same way observed for transition metals[1] (i.e., longer growth channels produce larger clusters). This behavior indicates that growth occurs primarily by condensation of atom and/or molecular species in the gas phase rather than by direct vaporization of clusters. Growth processes are so efficient that long growth channel lengths ($dl > 4$ cm) lead to depletion of atomic and small cluster species at the expense of larger aggregates. Thus, growth processes at the particular source conditions used are one important influence on mass spectra through effects on size dependent densities.

Small tin clusters: spectrometer focusing

Vaporization of a tin sample rod with a short cluster growth region ($dl = 1.0$ cm) only produces significant density for clusters up to 12–13 atoms. Figure 2 shows three different mass spectra taken under these conditions using high power ArF radiation (10 mJ/cm^2). These spectra were taken under the same nozzle source and ionization laser conditions but with different mass spectrometer focusing with deflection plates oriented along the molecular beam flight direction. As illustrated by these data, the deflection plates have a significant effect on the appearance of size distributions obtained in pulsed cluster beam experiments. This is a well-known phenomenon when the mass spectrometer flight tube is oriented perpendicular to the pulsed beam flight direction, as in our experiments. At the molecular beam velocity, different mass clusters have different kinetic energies and the deflection plates must compensate for this effect as cluster ions are turned into the flight tube. However, in spite of this broad focusing effect, local abundance maxima at $N = 8$ and 11 are clearly evident in all three spectra. An additional local minima at $N = 5$ is less pronounced, but does appear in the top two spectra. These local effects, which are properties of the cluster distribution rather than the mass spectrometer conditions, are the interesting data in mass spectral abundance patterns. To represent intensities in subsequent spectra in this paper, we have used averages of spectra under different focusing or selected spectra under representative focusing conditions.

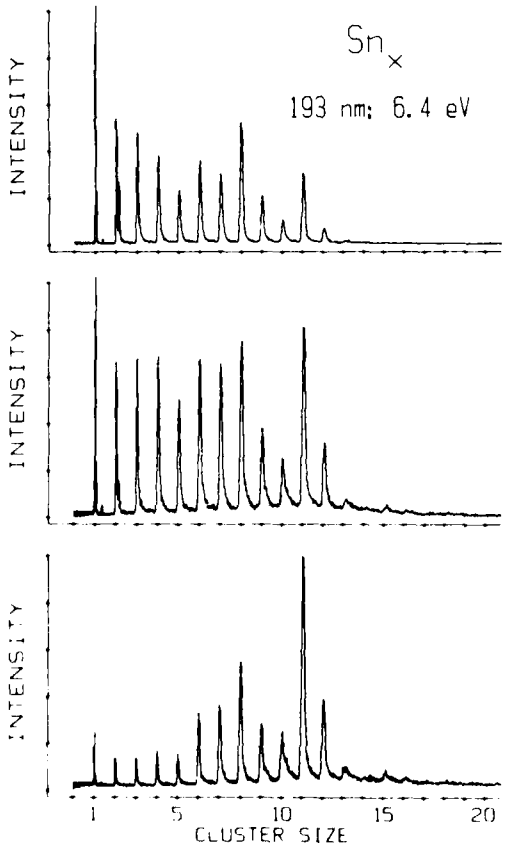

FIG. 2. Tin cluster mass spectra under different mass spectrometer focusing and laser timing synchronization conditions. Photoionization was accomplished at 193 nm (6.4 eV) with a fluence of 10 mJ/cm^2. At this high laser power, the abundant species indicated, which are independent of focusing, are most likely stable cations (i.e., Sn_8^+ and Sn_{11}^+).

The $N = 8$ and 11 maxima shown in Fig. 2 are only observed at the ArF wavelength at high laser powers. This data, together with the ionization potential information presented below, indicates that these features are caused by cluster fragmentation. Sn_8^+ and Sn_{11}^+, therefore, seem to be produced preferentially in the fragmentation of clusters in this size range and they are particularly resistant to further fragmentation at this wavelength.

Ionization thresholds and fragmentation

Figure 3 shows a power dependence study of tin clusters at 193 nm (6.4 eV). These data were obtained with a moderate length growth region on the cluster source ($dl = 2.0$ cm), producing larger clusters than those shown in Fig. 2. Interestingly, the maxima at $N = 8$ is not observed in the high power spectra at 193 nm when larger clusters are present. Apparently, the fragmentation processes of these additional clusters obscure the preferential formation of $N = 8$ cations, suggesting that they are formed primarily by fragmentation of smaller clusters.

As shown in Fig. 3, reducing the laser power has a dramatic effect on the tin cluster mass spectrum at 193 nm. Systematic power reduction causes the loss of cluster mass peaks below $N = 11$ and a relative increase in larger mass features, clearly indicating the effects of multiphoton absorption and fragmentation. After the power is reduced to the 0.025 mJ/cm^2 level, further reduction causes no further change in relative peak abundances and signals vary linearly with the laser power. Therefore, the data in the low power limit show cluster species that are ionized by single photon absorption and have ionization thresholds below the energy of the 6.4 eV photon. For tin, this condition applies to clusters containing 7 or more atoms. However, while cluster peaks for $N \geq 7$ are all observed in the low power limit, their intensities vary with cluster size. In particular, the $N = 7$–10 peaks have very low intensities compared to those for $N \geq 11$.

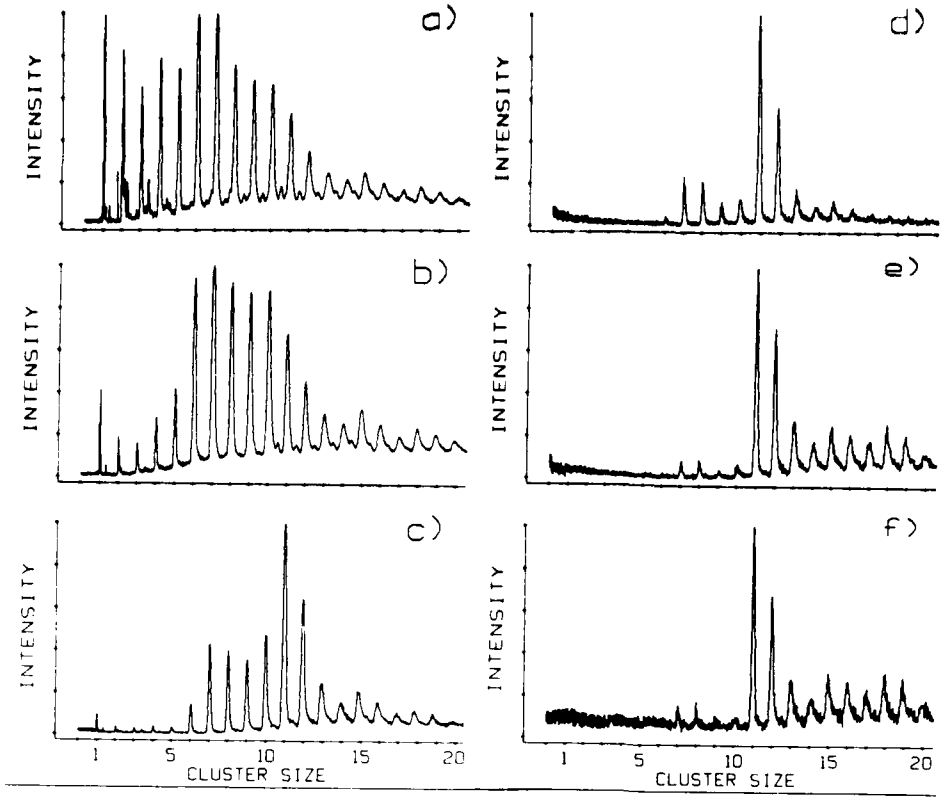

FIG. 3. Laser power dependent study of tin clusters at 193 nm. The laser powers corresponding to each spectra are: (a) 10.0 mJ/cm^2; (b) 5.0 mJ/cm^2; (c) 2.0 mJ/cm^2; (d) 0.5 mJ/cm^2; (e) 0.025 mJ/cm^2; (f) 0.012 mJ/cm^2. The effects of fragmentation at higher powers are clearly evident. In the low power limit (e) and (f) relative intensities do not change with further power reduction.

Since fragmentation is not expected under these conditions, these intensity variations must be caused by either the densities of different sized neutral clusters or by their relative cross sections for ionization at this wavelength. Only wavelength dependent photoionization can distinguish between these two alternatives.

Figure 4 shows the tin cluster mass spectra in the low power limit at 157 nm (7.9 eV) for comparison to the 193 nm data. Unfortunately, other photoionization wavelengths in this region are not available, but these spectra do clarify the effect of ionization cross sections. As shown, cluster peaks for $N \geqslant 11$ appear with nearly similar relative intensities in both 193 and 157 nm spectra. This is especially evident for peaks at $N = 11$ and 12 relative to larger species. The wavelength independence of this pattern suggests that intensities in this size region are caused by cluster densities rather than by ionization cross sections. However, cluster peaks in the 7 to 10-atom range, which are very weak in 193 nm spectra, have significantly greater intensity at 157 nm. The wavelength dependence of these features indicates that their intensities *are* affected by cross sections. Using tunable UV lasers, Kaldor and co-workers have shown that ionization cross sections for iron clusters are in many cases slowly rising functions of energy at threshold.[10] Thus, single photon ionization on the leading edge of a broad threshold may explain the low intensities for Sn_7–Sn_{10} in the 193 nm spectra. Interestingly, the mass peaks at $N = 7$ and $N = 10$ are especially prominent in this spectrum. A similar pattern is observed for lead clusters, as described below. These maxima could result from either enhanced densities in the 7 and 10-atom clusters or enhanced ionization cross sections for these species. Without additional wavelength dependent data for the 7–10-atom species, it is impossible to decide between these alternatives. Arguments presented below, however, favor enhanced density to explain these intensities. In the 1 to 6-atom size range, mass peaks which are not detected at 193 nm are all present in the 157 nm data. However, without photoionization at additional wavelengths for these species it is not possible to comment on the significance of their intensities.

In addition to the information provided about cross sections and abundance patterns, the data in Fig. 4 also makes it possible to bracket vertical ionization potentials (IPs) for tin clusters. Thus, for $N \geqslant 11$, IP's are less than 6.4 eV; for $N = 7$–10 they are very near, but just below 6.4 eV; and for $N = 1$–6 they are between 6.4 and 7.9 eV (note: this $N = 1$ determination is consistent with the known value of 7.34 eV). This data suggests a gradual falloff in IP with size, in qualitative agreement with the predictions of the classical metal droplet model.[22] However, detailed comparisons to

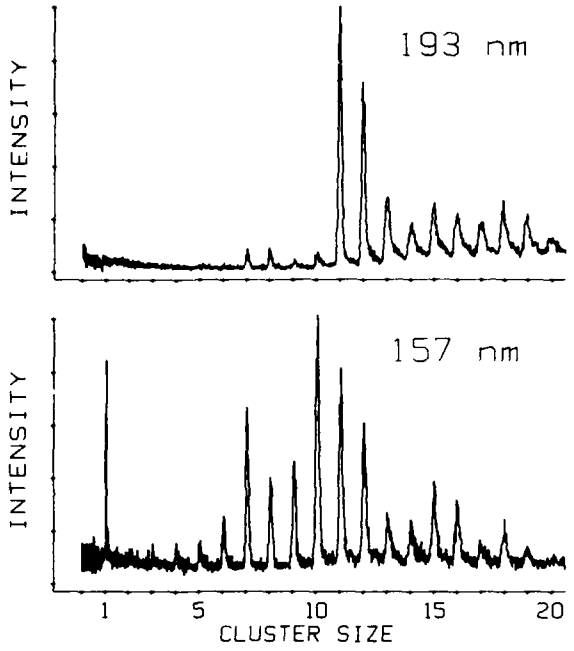

FIG. 4. Tin cluster mass spectra in the limit of low laser power at 157 nm (0.05 mJ/cm^2) and 193 nm (0.025 mJ/cm^2). These spectra show the onsets for single photon ionization at each wavelength and the relative cross sections for photoionization.

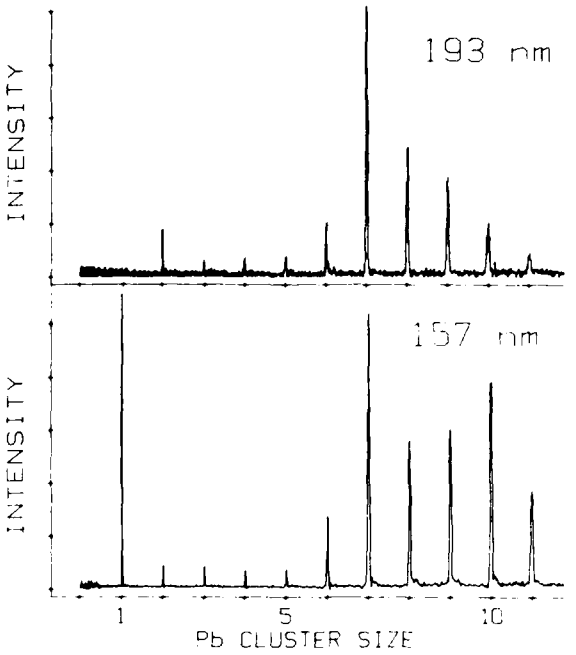

FIG. 5. Lead cluster mass spectra in the limit of low laser power at 157 nm (0.05 mJ/cm^2) and 193 nm (0.025 mJ/cm^2). All clusters are single photon ionized at both wavelengths.

this theory will require more accurate data from tunable laser experiments.

Lead cluster mass spectra show qualitatively the same fragmentation behavior observed for tin. At higher laser powers (193 nm) mass distributions favor smaller clusters and power reduction causes an increase in larger mass peaks. The mass spectral patterns in the limit of low laser powers are different from those of tin, however, because of specific ionization potentials and size dependent cross sections. Mass spectra in the low power limit at 193 and 157 nm are shown in Fig. 5. All clusters, but not the atom (IP = 7.42 eV) are observed at 193 nm and all clusters as well as the atom are observed at 157 nm. As observed for tin, relative intensities in the low power limit are invariant with laser power reduction and absolute intensities vary linearly with the power. Therefore, these data indicate that all lead clusters have ionization potentials below 6.4 eV. This upper limit is consistent with IP values for Pb_2-Pb_5 measured by electron impact of lead species in equilibrium with the solid in an oven (Pb_2: 6.2 eV; Pb_3: 5.8 eV; Pb_4: 5.7 eV; Pb_5: 5.7 eV; Pb_6: 5.48 eV; Pb_7: 5.3 eV).[19]

As shown in Fig. 5, there are significant similarities in the lead abundance patterns at the two different wavelengths. Both mass spectra have an overall contour peaked in the general region of $N = 6$–10, while the $N = 2$–5 mass features have relatively low intensities. Additionally, both mass spectra have a local maxima at $N = 7$. The wavelength independence of the $N = 7$ feature and the overall contours of the two spectra suggest that these intensities are caused by relative cluster densities rather than by ionization cross sections. The $N = 10$ mass peak, which is a relative maxima in the 157 nm spectrum but not in the 193 nm spectrum, is an exception to this general statement. The wavelength dependence of this feature makes it impossible to separate the influences of cluster density and relative ionization cross sections.

One important caveat in all the lead cluster mass spectra is the dependency of mass spectra on the nozzle geometry. For example, Fig. 6 shows a lead cluster spectrum, using low power ionization at 193 nm, with a growth channel length 1 cm longer than that used for the data in Fig. 5. In the longer growth region, condensation has proceeded to the point that smaller clusters ($N = 2$–6) are virtually absent from the

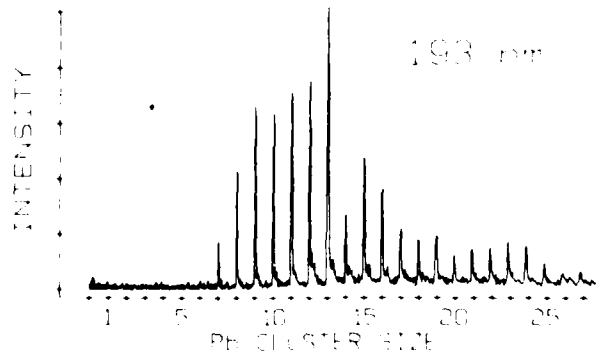

FIG. 6. Lead cluster mass spectrum at 193 nm (1 mJ/cm^2 power) the nozzle source growth region is extended. Smaller clusters are absent because they have condensed to form larger species.

molecular beam. Consequently, the relative maxima at $N = 7$ observed in Fig. 5 is not seen under these conditions, and it is replaced by a relative maxima at $N = 13$. Without complete studies of growth channel conditions, data such as these would completely confuse estimates of ionization potentials, etc. Both tin and lead clusters were studied under a variety of nozzle conditions, at both ionization wavelengths, to account for these effects.

Abundance patterns under limiting conditions

With information about ionization thresholds, cross sections, and fragmentation, it should be possible to choose photoionization conditions which probe the relative densities of neutral clusters in the molecular beam. Our power dependent mass spectral data at 193 and 157 nm provide good estimates of ionization potentials and the effects of fragmentation. However, Figs. 4 and 5 show that both tin and lead spectra are influenced by wavelength dependent ionization cross sections. While some features in these spectra are wavelength independent (e.g., the Pb_7 maximum), it is clear that detailed conclusions about relative cluster concentrations cannot be reached with photoionization at only two wavelengths. Even without full wavelength dependent photoionization studies, however, some qualitative insights into relative cluster densities are possible with the existing data. With the exception of small tin clusters ($N = 2$–6), all the species studied here have ionization potentials less than or equal to 6.4 eV. The 7.9 eV ionization (at 157 nm) therefore must be at least 1.5 eV above threshold for all these clusters. Ionization cross sections for more conventional small molecules vary most near threshold and become smoother functions toward higher energy.[23] If metal clusters follow this same behavior, then ionization at 7.9 eV would be expected to provide spectra less affected by cross section variations and more nearly reflecting cluster densities. Of the ionization conditions available here, then, low power radiation at 157 nm provides the best opportunity to probe neutral cluster densities.

Figure 7 shows a comparison of tin and lead clusters under our best approximation to "neutral sensitive" conditions (157 nm; 0.1 mJ/cm^2). The two spectra are qualitatively similar in several respects. Both exhibit broad maxima for cluster peaks in approximately the 6 to 15-atom range. Both also exhibit clear local maxima at $N = 7$ and 10. Neither distribution contains significant intensities for larger clusters ($N \gtrsim 20$). While these common features may be caused by local ionization cross sections, such effects 1.5 eV above threshold causing tin and lead distributions to look so similar seems to be an unlikely coincidence. It is more likely that these spectra reflect true similarities in tin and lead relative cluster densities. More noticeable differences are observed when peak intensities are considered in more detail. The lead distribution, for example, exhibits a slight but reproducible maxima at $N = 13$ which is not observed for tin but is also observed in lead spectra at 193 nm (Fig. 6). In fact, Sn_{11}, Sn_{14}, Sn_{17}, Pb_9, Pb_{14}, Pb_{18}, and Pb_{20} mass peaks are all local minima. Thus, there seem to be both similarities and distinct differences between the mass distributions for neutral tin and lead clusters.

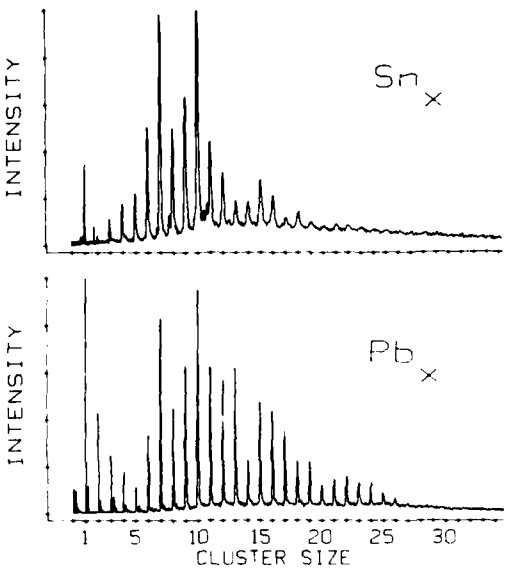

FIG. 7. A comparison of tin and lead clusters under conditions (157 nm; 0.1 mJ/cm^2) selected to ionize neutrals without substantial fragmentation ("neutral sensitive conditions"). Maxima shown in both distributions are at $N = 7$ and $N = 10$.

Although mass spectra clearly do not measure cluster structure, it is always interesting to speculate on the structures of special clusters suggested by these data. As discussed below, the lead cluster mass spectrum described here closely resembles that produced in previous experiments under different conditions.[2,4] In particular, the pattern of a maximum at $N = 13$ and 19, and minima at $N = 14$, 18, and 20 is a familiar one and has been observed previously in mass spectra of rare gas atom van der Waals clusters.[24] An additional maximum at $N = 17$ has been observed in previous lead experiments.[4] Maxima at $N = 17$ and 19 are not clearly evident in Fig. 7, but do become prominent under other photoionization conditions described below. This overall pattern has been explained by a simple atom close-packing model built on stable 13-atom icosahedral and 19-atom double icosahedral structures.[4] Minima in abundances are then expected for structures one atom beyond or one atom short of a stable unit. The 7-atom unit is related to this structural scheme and can be rationalized as a half-completed icosahedron in the form of a pentagonal bipyramid.[12] Neither the 17-atom structure nor the 10-atom unit in these clusters are predicted by sphere packing models.[4] Phillips[12] has used an analogy with calculated silicon structures to predict an adamantane cage structure (a fragment of the solid diamond lattice) for Ge_{10}, and this reasoning could be extended to Sn_{10} and Pb_{10}. King, on the other hand, has used graph theory and topology arguments, as well as comparisons to condensed phase clusters of tin or lead with known structures, to consider the $N = 7$ and 10 features in our data.[25] He suggests a capped octahedron for the 7-atom species (C_{3v} symmetry) and a 3,4,4,4-tetracapped trigonal prism for the 10-atom species. King's suggestions are supported to some degree by recent *ab initio* calculations of silicon clusters by

Tomanek and Schlüter[26] which suggest the tetracapped trigonal prism to be substantially more stable than the diamond-lattice fragment. The two proposed structures for the 10 atom cluster are shown in Fig. 8. The most significant difference in these structures is that the diamond-lattice fragment necessarily has "dangling" unused orbitals while the capped trigonal prism uses more bonding capacity in covalent interactions.

For comparison to the mass spectra at low laser power, Fig. 9 shows a comparison of tin and lead clusters under high power photoionization conditions (193 nm; 10 mJ/cm^2). Based on the results of power dependences, these spectra are known to be the result of severe multiphoton absorption and fragmentation. Thus, abundances favor stable *cations* which are formed preferentially in fragmentation or which are resistant to further fragmentation. Both cluster distributions differ markedly from those under neutral sensitive conditions. For example, the maxima at $N = 7$ and 10 are essentially gone, confirming their assignment to neutral cluster species. Additionally, both metals have enhancements at lower mass peaks, as expected from fragmentation. At higher masses, however, the tin cluster distribution drops off abruptly in intensity near $N = 10$–12, while the overall lead distribution falls off slowly out to beyond $N = 30$–40. The presence of such large lead clusters under these conditions is surprising, since low power spectra at either 193 nm or 157 nm do not extend to these higher masses. Ionization potentials of these larger lead clusters should certainly be lower than those in the 2 to 10-atom range. Thus, lead clusters in the 20–40 atom size range must have a lower ionization cross section than smaller clusters for single photon absorption, but can be detected under high fluence multiphoton absorption conditions. Under these high fluence conditions, the ionization of smaller clusters has probably saturated, resulting in an apparent increase in intensity of the larger clusters. The tin distribution, however, does not include these larger clusters under any laser fluence conditions. In addition to these broad effects, both cluster distributions also have local maxima and minima under these conditions. Patterns in the tin distribution in the region of $N = 12$–20 are very similar to the corresponding "neutral" spectrum except that $N = 14$ is slightly more depleted. However, the lead pattern associated with close-packed structures is dramatically more pronounced than in the neutral data. Enhancement in this pattern at high laser powers is understandable because the minima in these patterns are associated with clusters containing one more atom than stable structures at $N = 13$, 17, or 19.[4] Under multiphoton absorption, clusters experience internal heating, and fragmentation resembles thermal evaporation. The most external atoms, such as those bound to an otherwise closed structure, evaporate most easily, thus depleting the corresponding mass channels. This heating effect should be essentially wavelength independent. Figure 10 shows a similar lead cluster distribution under high power radiation

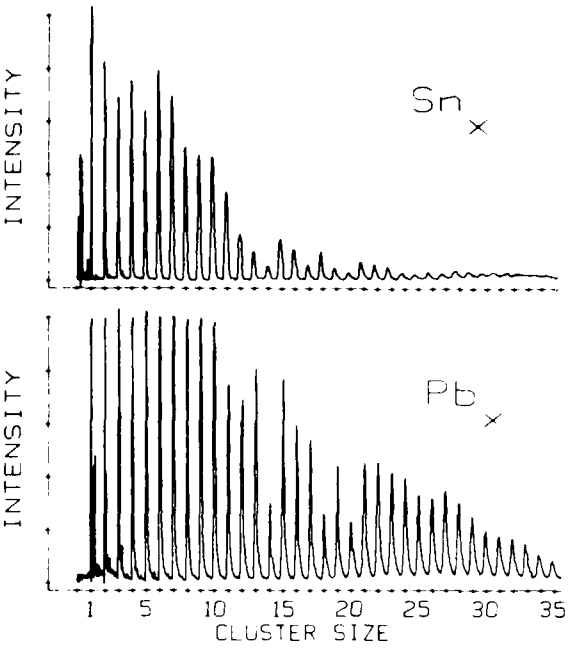

FIG. 9. A comparison of tin and lead cluster mass spectra under conditions (193 nm; 10.0 mJ/cm^2) chosen to induce fragmentation by multiphoton absorption ("cation sensitive conditions").

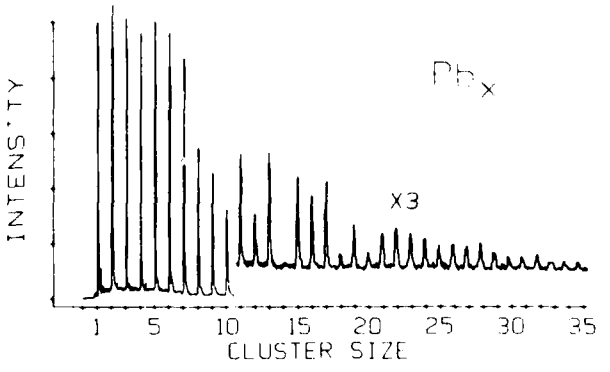

FIG. 10. Lead cluster mass spectrum at 248 nm (KrF radiation, 18 mJ/cm^2). By comparison to the lead spectra in Fig. 7, this data illustrates the wavelength independence of cation forming conditions and the enhancements in the mass spectral pattern associated with close-packed structures.

FIG. 8. Two proposed structures for the 10-atom cluster observed for silicon, germanium, tin, and lead. (a) is the adamantane-like diamond lattice fragment. (b) is the 3,4,4,4-tetracapped trigonal prism.

at 248 nm (KrF excimer laser; 4.99 eV; 18 mJ/cm^2) which confirms this idea. At this longer wavelength and higher power, the distribution is more highly fragmented than that shown in Fig. 9 and the pattern of minima at $N = 14$, 18, and 20 is even more pronounced. The increased importance for this close-packing pattern for lead under these conditions suggests that tin and lead cations produced by MPI fragmentation may not be as similar as the corresponding neutrals produced initially in laser vaporization. Another possible explanation is that the heating caused by multiphoton absorption "anneals" the clusters and they reform into more stable structures than those formed initially. If this is true, then close-packed structures built around icosahedral units may be more stable than covalently bonded species like the recurring 10-atom unit.

It is interesting to compare these data to previous tin and lead experiments, where both neutral and cation clusters were pr duced and detected by different methods. In the case of lead, Sattler and co-workers produced clusters using inert gas condensation in an oven source and detected them with electron impact ionization (35 eV).[2,4] Surprisingly, their mass spectral data contain local maxima at 7, 10, and 13 as well as minima at 14, 18, and 20, in agreement with our photoionization data in Fig. 7. Although the close-packing pattern is more pronounced in the Sattler data, it is otherwise the same as that taken under our neutral favoring conditions. Martin and Schaber have studied tin clusters up to $N = 16$ using a similar oven/beam source at higher electron impact energies (70 eV).[5] These data do no. produce the $N = 7$ and $N = 10$ maxima in our Fig. 7 data, but instead resemble our data under high power laser conditions in Fig. 9. High energy electron beam ionization would be expected to cause extensive fragmentation just like high power laser radiation. The Sattler data show, however, that lower energy electron impact ionization can produce the same results obtained with low power photoionization. Allowing for the understandable detection differences, then, this comparison suggests that laser vaporization and inert gas condensation methods both produce essentially the same relative size distributions of tin and lead clusters. Both sources grow clusters primarily by single atom addition, but other conditions such as buffer gas temperature and the possible involvement of ions (only in the laser vaporization source) are very different. This insensitivity to source conditions suggests that abundance patterns must be strongly influenced by the relative thermodynamic stability of the clusters formed within the framework of growth by single atom addition. It is conceivable, however, that more stable species might be preferred if there were enough energy for internal reorganization following each atom addition.

It is also useful to compare tin and lead systems to clusters of other group IVA elements (C, Si, Ge). Because of higher ionization potentials relative to available lasers, carbon and silicon clusters have not been studied with single photon ionization.[6,16,21] However, higher laser powers under fragmented conditions produce maxima for C_{11} and C_{15},[16] and for Si_6, Si_7, Si_{10}, and Si_{11}.[6,21] Smalley and coworkers have noted the strong similarities between silicon and germanium cations,[6] especially with respect to the maxima at $N = 6$ and 10. Our tin data in Fig. 9 also shows some evidence for this pattern. The germanium cation data of Bloomfield, Freeman, and co-workers,[27] under slightly different conditions than those presented by Smalley, show minima at $N = 13$, 17, and 20 which are also reflected to some extent in our tin data. This germanium cation pattern is also produced in Ge cluster mass spectra with 70 eV electron impact ionization.[5] Low power radiation at 157 nm (neutral conditions) produces maxima for Ge_6 and Ge_{10}^6 for comparison to our lead and tin maxima at $N = 7$ and 10. Therefore, special cation or neutral species with 6, 7 or 10 atoms seem to be general characteristics of Group IVA clusters. Interestingly, 10-atom germanium or silicon clusters are observed when anion or cation clusters are sampled directly from the laser vaporization source[28] (i.e., Ge_{10}^-, Ge_{10}^+), as well as from photoionization or electron impact ionization of neutrals. In other work in our laboratory we have also observed an enhanced abundance for the cluster In_5Bi_5 which also has ten atoms and is isoelectronic to the group IVA neutral 10-atom species.[29]

Underlying the common traits in Group IVA clusters, there seems to be a gradual trend in bonding properties proceeding down the periodic table. Carbon clusters are significantly different in their abundance patterns from silicon clusters. Silicon and germanium cation distributions are almost identical.[6] Germanium cluster distributions under neutral conditions have maxima at Ge_6 and Ge_{10}, which have switched over to maxima at $N = 7$ and 10 for tin. Germanium and tin cations, however, both have maxima at $N = 6$ and 10 as well as minima at $N = 13$, 17, and 20. Tin clusters have an additional minima at $N = 14$ not observed for germanium, but which is one of the main features in the close-packing pattern observed for lead. Neutral lead and tin clusters both have the same 7 and 10 pattern but lead has the more pronounced features associated with close packing. This close-packing pattern is completely dominant in lead cations, but there is only a hint of this tendency for tin (slight minimum at $N = 14$). A variety of factors could contribute to these trends. Similarities, of course, are easiest to attribute to the common number of valence electrons. Atomic size arguments, which may be important in forming optimum polyhedral networks, would group carbon by itself, silicon and germanium more nearly together, and tin and lead together. Ionization potentials decrease down the group with greater breaks between carbon and silicon and between germanium and tin. Electron affinities also decrease more smoothly down the group with the greatest break between tin and lead. Relativistic effects, which would weaken covalent bonding tendencies,[17] are expected to a limited degree for tin and should become most important for lead. The importance of close-packing structures for lead is consistent with this latter idea, since close-packing structures should become more important when covalent bonding interactions are weakened. Interestingly, similar trends are observed in the bulk solids of these materials.[30] Graphitic carbon is very different in structure from silicon or germanium, but both silicon and germanium have the diamond lattice solid structure. Solid tin has properties intermediate to those of germanium and lead. α-Sn, which is stable as a gray semimetal,

crystallizes at low temperature in the same diamond lattice observed for germanium. At high temperature, tin exists in the white metallic form (β-Sn) in which atoms are more densely packed. In lead, covalent interactions are at a minimum and the solid exists in the cubic close-packed structure.

Unfortunately, the observations and conclusions about cluster structure based on our mass spectral data must remain very tentative. However, in the immediate future, no direct measures of cluster structure appear to be available. Optical spectroscopy experiments have still not been demonstrated for any cluster larger than three atoms. Recent developments have made photoelectron spectroscopy feasible in cluster beam experiments,[38,39] but this technique provides a better probe of electronic structure than it does of geometry. Quantum chemistry calculations testing cluster stability show some promise. These calculations have already been extended to 10–15-atom species of carbon and silicon,[31-34] and they are not far out of reach for germanium, tin, and lead. For example, Hückel molecular orbital calculations have been performed for 9-atom tin and lead cluster anions,[35,36] and *ab initio* methods using relativistic effective core potentials have been demonstrated for smaller tin and lead species.[37] Until more refined optical spectroscopy and/or theory techniques become available, continued mass spectroscopy experiments with careful attention to photoionization dynamics seems to be the most productive approach to the study of larger clusters.

CONCLUSION

We have described UV laser photoionization experiments on tin and lead cluster species produced by laser vaporization. Through laser wavelength and power dependence studies of mass spectra, it is possible to elucidate the effects of ionization potentials, fragmentation, and, to a limited degree, relative ionization cross sections. Considering these effects, conditions can be adjusted to probe neutral cluster abundances and fragmented cluster cation abundances. The comparisons to other Group IVA clusters suggest similarities in cluster properties that are common to several group members and systematic variations in properties through the group. To our knowledge, this data and the comparison to previous related data provides the first systematic view of periodic cluster properties. The trends apparent in these data suggest that both experimental and theoretical cluster research could benefit from further systematic studies of isoelectronic clusters of the main group elements.

ACKNOWLEDGMENTS

The authors wish to thank Professor R. B. King for helpful discussions related to this work. This research was supported by the U.S. Army Research Office through contract number DAAG-85-K-0040. Additional support was received from the Office of Naval Research.

[1](a) T. G. Dietz, M. A. Duncan, D. E. Powers, and R. E. Smalley, J. Chem. Phys. **74**, 6511 (1981); (b) J. B. Hopkins, P. R. R. Langridge-Smith, M. D. Morse, and R. E. Smalley, *ibid.* **78**, 1627 (1983).
[2](a) K. Sattler, J. Mühlbach, and E. Recknagel, Phys. Rev. Lett. **45**, 821 (1980); (b) J. Mühlbach, P. Pfau, K. Sattler, and E. Recknagel, Z. Phys. B **47**, 233 (1982).
[3]W. D. Knight, K. Clemenger, W. A. DeHeer, W. A. Saunders, M. Y. Chow, and M. L. Cohen, Phys. Rev. Lett. **52**, 2141 (1984).
[4]J. Mühlbach, K. Sattler, P. Pfau, and E. Recknagel, Phys. Lett. A **87**, 415 (1982).
[5]T. P. Martin and H. Schaber, J. Chem. Phys. **83**, 855 (1985).
[6]J. R. Heath, Y. Liu, S. C. O'Brien, Q. L. Zhang, R. F. Curl, F. K. Tittel, and R. E. Smalley, J. Chem. Phys. **83**, 5520 (1985).
[7](a) M. E. Geusic, M. D. Morse, S. C. O'Brien, and R. E. Smalley, J. Chem. Phys. **82**, 590 (1985); (b) M. D. Morse, M. E. Geusic, J. R. Heath, and R. E. Smalley, *ibid.* **83**, 2293 (1985).
[8](a) R. L. Whetten, D. M. Cox, D. J. Trevor, and A. Kaldor, Phys. Rev. Lett. **54**, 1494 (1985); (b) D. J. Trevor, R. L. Whetten, D. M. Cox, and A. Kaldor, J. Am. Chem. Soc. **107**, 518 (1985).
[9]S. C. Richtsmeier, E. K. Parks, K. Liu, L. G. Pobo, and S. J. Riley, J. Chem. Phys. **82**, 3659 (1985).
[10](a) E. A. Rohlfing, D. M. Cox, A. Kaldor, and K. Johnson, J. Chem. Phys. **81**, 3846 (1984); (b) R. L. Whetten, M. R. Zakin, D. M. Cox, D. J. Trevor, and A. Kaldor, *ibid.* **85**, 1697 (1986).
[11]L. S. Zheng, C. M. Karner, P. J. Brucat, S. H. Yang, C. L. Pettiette, M. J. Craycraft, and R. E. Smalley, J. Chem. Phys. **85**, 1681 (1986).
[12]J. C. Phillips, Chem. Rev. **86**, 619 (1986).
[13]E. Schumacher, M. Kappes, K. Marti, P-Radi, M. Schär, and B. Schmidhalter, Ber. Bunsenges. Phys. Chem. **88**, 220 (1984).
[14]J. Bernholc and J. C. Phillips, J. Chem. Phys. **85**, 3258 (1986).
[15](a) R. G. Wheeler, K. LaiHing, W. L. Wilson, and M. A. Duncan, Chem. Phys. Lett. **131**, 8 (1986); (b) R. G. Wheeler, K. LaiHing, W. L. Wilson, J. D. Allen, R. B. King, and M. A. Duncan, J. Am. Chem. Soc. **108**, 8101 (1986).
[16]E. A. Rohlfing, D. M. Cox, and A. Kaldor, J. Chem. Phys. **81**, 3322 (1984).
[17](a) K. Pitzer, Acc. Chem. Res. **12**, 271 (1979); (b) P. Pyykko and J. P. Desclaux, *ibid.* **12**, 276 (1979).
[18]R. G. Wheeler and M. A. Duncan, J. Phys. Chem. **90**, 1610 (1986).
[19]Y. Saito, K. Yamauchi, K. Mihama, and T. Noda, Jpn. J. Appl. Phys. **21**, L396 (1982).
[20]P. J. Brucat, L. S. Zheng, C. L. Pettiette, S. Yang, and R. E. Smalley, J. Chem. Phys. **84**, 3659 (1986).
[21](a) L. A. Bloomfield, R. R. Freeman, and W. L. Brown, Phys. Rev. Lett. **54**, 2246 (1985); (b) L. A. Bloomfield, M. E. Geusic, R. R. Freeman, and W. L. Brown, Chem. Phys. Lett. **121**, 33 (1985); (c) M. E. Geusic, T. J. McIlrath, M. F. Jarrold, L. A. Bloomfield, R. R. Freeman, and W. L. Brown, J. Chem. Phys. **84**, 2421 (1986).
[22]D. M. Wood, Phys. Rev. Lett. **46**, 749 (1981).
[23]J. Berkowitz, *Photoabsorption, Photoionization, and Photoelectron Spectroscopy* (Academic, New York, 1979).
[24]O. Echt, K. Sattler, and E. Recknagel, Phys. Rev. Lett. **47**, 1121 (1981).
[25]R. B. King in *Proceedings of the International Symposium on the Physics and Chemistry of Small Clusters* (Plenum, New York, 1987).
[26]D. Tomanek and M. A. Schlüter, Phys. Rev. Lett. **56**, 1055 (1986).
[27]J. C. Phillips, J. Chem. Phys. **85**, 5246 (1986).
[28]Y. Liu, Q.-L. Zhang, F. K. Tittel, R. F. Curl, and R. E. Smalley, J. Chem. Phys. **85**, 7434 (1986).
[29]M. Bishop, K. LaiHing, and M. A. Duncan (unpublished).
[30]J. S. Blakemore, *Solid State Physics* (Cambridge University, Cambridge, 1985).
[31]H. Hintenberger, J. Franzen, and K. D. Schuy, Z. Naturforsch. Teil A **18**, 1236 (1963).
[32]R. Hoffman, Tetrahedron **22**, 521 (1966).
[33]D. W. Ewing and G. V. Pfeiffer, Chem. Phys. Lett. **86**, 365 (1982).
[34](a) K. Raghavachari and V. Logovinsky, Phys. Rev. Lett. **55**, 2853 (1985); (b) K. Raghavachari, J. Chem. Phys. **84**, 5672 (1986).
[35]L. L. Lohr, Inorg. Chem. **20**, 4229 (1981).
[36]R. C. Burns, R. J. Gillespie, J. A. Barnes, and M. J. McGlinchey, Inorg. Chem. **21**, 799 (1982).
[37](a) K. Balasubramanian, J. Chem. Phys. **85**, 3401 (1986); (b) K. Balasubramanian and K. S. Pitzer, *ibid.* **78**, 321 (1983).
[38]D. G. Leopold, J. Ho, and W. C. Lineberger, J. Chem. Phys. **86**, 1715 (1987).
[39]O. Cheshnovsky, P. J. Brucat, S. Yang, C. L. Pettiette, M. J. Craycraft, and R. E. Smalley, *Proceedings of the International Symposium on the Physics and Chemistry of Small Clusters* (Plenum, New York, 1987).


FILMED
68